



Numerical modeling of a tunnel in jointed rocks subjected to seismic loading

Malavika Varma^{*}, V.B. Maji, A. Boominathan

Department of Civil Engineering, Indian Institute of Technology Madras, Chennai, India

Received 9 May 2018; received in revised form 20 September 2018; accepted 2 November 2018

Available online 21 December 2018

Abstract

The studies on the performance of tunnels under static loads are reported extensively in the literature but their performances under dynamic loads are limited. The present study highlights some of the important aspects of jointed rock tunnels during seismic loading. The literature review provides a shake table experimental study of a jointed rock tunnel. A Universal Distinct Element Code (UDEC) model is developed from this shake table experiment. The model tunnel is subjected to a scaled input motion of the 1985 Mexico earthquake. The numerical results are validated systematically with the findings of the shake table experiment. Further, the developed numerical model is used to perform parametric studies to understand the effect of in-situ stress, joint angles, joint stiffness, and joint friction angle on the deformation and stability of the tunnel under the same earthquake input motion. It is observed that some joint angle combinations form a wedge that yields excessive deformation and subsequently a complete failure. An exponential decrease in deformation occurred in the tunnel as the joint stiffness increases. It is found that the shallow tunnels are more susceptible to damage under the action of earthquake loads.

© 2018 Tongji University and Tongji University Press. Production and hosting by Elsevier B.V. on behalf of Owner. This is an open access article under the CC BY-NC-ND license (<http://creativecommons.org/licenses/by-nc-nd/4.0/>).

Keywords: Tunnel; Jointed rocks; Seismic loading; UDEC

1 Introduction

The development of various infrastructure projects currently are closely linked with underground structures, such as utility tunnels, Metro Rail Transport System, hydropower caverns, or nuclear repositories. Therefore, the stability and performance of tunnels must be studied. Tunnels built in rocks are always assumed to be strong and stable. Its performance under seismic condition is hardly analyzed. However, the failures of tunnels under seismic loading have been reported in the literature (Dowding & Rozen, 1978; Kaneshiro, Power, & Rosidi, 2000; Owen & Scholl, 1981; Power, Rosidi, & Kaneshiro,

1998; Sharma & Judd, 1991). Hence, it is important to study the effect of seismic loading on tunnels. In most of these studies, damages in rock tunnels occurred via a pre-existing discontinuity that acted as a guiding medium for further damage. The discontinuity may occur in the form of faults, joints, folding, infilling, or any other type of anisotropy that yields weakness. Among these, joints are the most typical and unavoidable, with high uncertainties regarding its properties resulting in uncertainties in rock behaviors. A jointed rock tunnel stable under static conditions may or may not exhibit the same behavior under the action of dynamic loads. Therefore, it becomes important to study the performance of rock jointed tunnels under seismic action. The present study attempts to understand the factors on which the tunnels under earthquake loading might be stable or unstable, and to propose simple measures that can be adopted to avoid tunnel failure.

^{*} Corresponding author.

E-mail address: malavikavarmamail@gmail.com (M. Varma).

The earliest consideration of seismic load on underground structures was performed by Barton (1984) using the Q system of the rock mass classification, assuming that Q_{seismic} is half of Q_{static} . Subsequently, during the planning of nuclear waste repository projects in the United States, several studies were conducted to understand the behavior of joints under seismic conditions (Ahola, Hsu, & Kana, 1996; Kana, Vanzant, Nair, & Brady, 1991; Kana, Fox, Hsu, & Chowdhury, 1997). The studies were primarily based on the deep mining area of the Lucky Friday mine. Ahola et al. (1996) performed shake table experiments to obtain the response of a circular tunnel in jointed medium and identify tunnel failure by the rock slip acting along the joints. It was found that for jointed rocks, the joint displacements are cumulative for recursive loading. Adyan and co-workers also conducted model tests on breakable and unbreakable blocks using a one-dimensional shake table (Adyan, 1994; Adyan & Kawamoto, 2004; Genis & Adyan, 2002, 2008; Adyan, Ohata, Genis, Tokashiki, & Ohkubo, 2010). These experiments are primarily focused on shallow unsupported tunnels. Dhawan, Singh, and Gupta (2004), Abokhalil (2007), Yoo, Park, Park, and Lee (2017), Adyan et al. (2010) have also identified the effect of underground structures in rocks to understand their performances under seismic conditions. While Dhawan et al. (2004) used the actual earthquake data of the Koynanagar earthquake (1967) for multiple underground openings for a dam, Abokhalil (2007) used pseudo-static methods. Both studies were performed using finite element analysis with plastic behavior consideration for the rock. It was concluded that plastic damage occurs near the underground opening, which was not transmitted to the surface or other parts.

Some studies not being limited to seismic loading focused on the tunnel response under other types of dynamic loading such as blast loading and rock bursts (Deng et al., 2014; Heuze & Morris, 2007; Rosengren, 1993; Wang, Li, & Shen, 2007). In most of these studies, the effect of joints around the tunnel when a shock load was applied at the surface was analyzed. All the studies above confirmed that the discontinuities present in the rock act as a guiding medium for further damages, joint slips, or any deformations. However, the effect of different geological parameters is still unexplored.

In the present study, a shake table experimental study of a tunnel in jointed rocks reported by Ahola et al. (1996) is modeled using the Universal Distinct Element Code (UDEC). The tunnel was subjected to a scaled input motion of the 1985 Mexican earthquake. The numerical results are validated with the findings of the shake table experiments. Further, the developed numerical model is used to perform parametric studies to understand the effect of joint angles, joint stiffness, in-situ stress, and joint friction angle on the deformation and stability of the tunnel under the same earthquake input motion. Tunnel failures found in the study are primarily by joint slippage through the existing discontinuities.

2 UDEC formulation

To represent discontinuities, Cundall (1971) formulated a distinct element method (DEM) that uses the discontinuous method of analysis. The DEM is an explicit time-marching method in which the blocks can be considered as rigid or deformable bodies and the contacts as deformable.

In the UDEC, each block considered to be a continuum is analyzed using the finite difference method of analysis by constant strain triangles and the corresponding discontinuity using boundary conditions. A step-by-step stress relaxation technique is adopted for the UDEC analysis, which alternates between Newton's equation of motion and stress displacement law. The relaxation process can be defined as the cycle of calculations between stress equations and equations of motion for each time step.

The operating cycle primarily depends on the assumption of the blocks as rigid or deformable (Fig. 1). The definition of the block as rigid or deformable determines the calculation process performed in the program. For rigid blocks, the force and displacement calculations are performed at the center of the block. The force and displacement are calculated as follows, respectively:

$$F_i = \sum F_i^c \quad (1)$$

$$\ddot{u} = \frac{F_i}{m} \quad (2)$$

where F_i^c is the force at the contact interface and m is the mass of the block under consideration. In the case of deformable blocks, the analysis is conducted for each zone element. Triangular zone elements used in the UDEC eliminates the error owing to hourglass deformation. The motion of each vertex of the triangular zone (grid point) is calculated by considering a Gaussian surface along the block

$$\ddot{u} = g_i + \frac{\int_s \sigma_{ij} n_j ds + F_i}{m_i} \quad (3)$$

where s is the surface enclosing the mass, m_i is lumped at the grid point, F_i is the resultant of all external forces applied to the grid point (which will be zero for the static condition), n_j is the unit normal to s , and g_i is the acceleration owing to gravity.

On the application of dynamic loads, the equation of motion with damping is considered. The relaxation method used in the dynamic solution scheme is shown in Fig. 2. The excessive energy at the contacts is absorbed and the steady-state solution is obtained. The calculation cycle in the dynamic consideration is similar to the static case with the only difference in the pattern of block relaxation. In dynamic loads, the blocks are relaxed successively and individually; meanwhile in static loads, successive relaxation is used.

This modeling method has disadvantage in calculating contact overlap and joint contacts, known as the contact

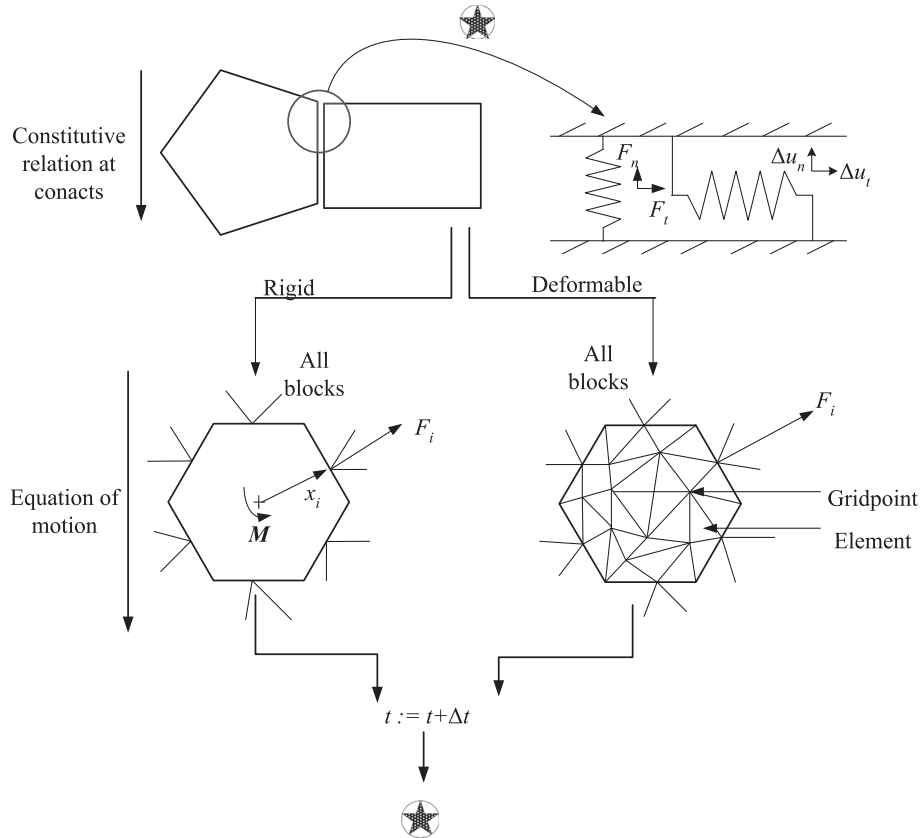


Fig. 1. Calculation cycle of UDEC (after Hart, 1993).

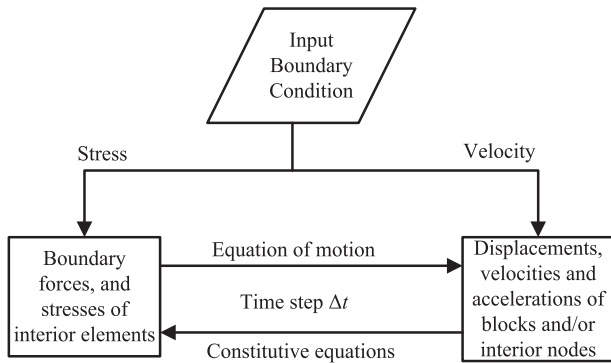


Fig. 2. Relaxation method for dynamic condition adopted Itasca (2014).

overlap error (Fig. 3). The interaction and loading between two adjacent blocks are determined by the minimum distance between the adjacent blocks, which is established numerically. The contact type, maximum gap, and sliding plane of two joints are determined by a contact detection algorithm. The joint stiffness defined between the blocks in normal and tangential directions determines the mechanical calculations performed at the contacts, as in Fig. 3. The interaction forces developed in the normal and tangential directions (F_n and F_t) of the contact points determine the relative displacements that these blocks undergo (u_n and u_t) and are represented as follows:

$$\Delta F_n = K_n \Delta u_n \tag{4}$$

$$\Delta F_t = K_t \Delta u_t \quad \text{NoSlip} \tag{5}$$

$$\Delta F_t = \Delta F_n \tan \Phi \quad \text{Slippage} \tag{6}$$

The contact surfaces may occur as a vertex-to-edge contact or an edge-edge contact (combination of numerous vertex-to-edge contacts). A linear or nonlinear relation can express the slippage between the contact surfaces such as the Mohr–Coulomb model, continuously yielding model, or Barton–Bandis model. The stress displacement relations for a simple Coulomb friction for these contacts are established as follows:

$$\Delta \sigma_n = k_n \Delta u_n \tag{7}$$

$$\Delta \sigma_t = k_t \Delta u_t \quad \text{NoSlip} \tag{8}$$

$$\Delta \sigma_t = \Delta \sigma_n \tan \Phi \quad \text{Slippage} \tag{9}$$

where Δu_n represents the interpenetration of the blocks known as the contact overlap between the adjacent blocks in the normal direction. Cohesion is always assumed to be zero when slippage occurs. If the contact overlap exceeds the prescribed tolerance limits, the calculations terminate with the contact overlap error.

3 Tunnel subjected to seismic motion

To understand the behavior of the joints around a tunnel under dynamic loads, the dynamic analysis of a tunnel

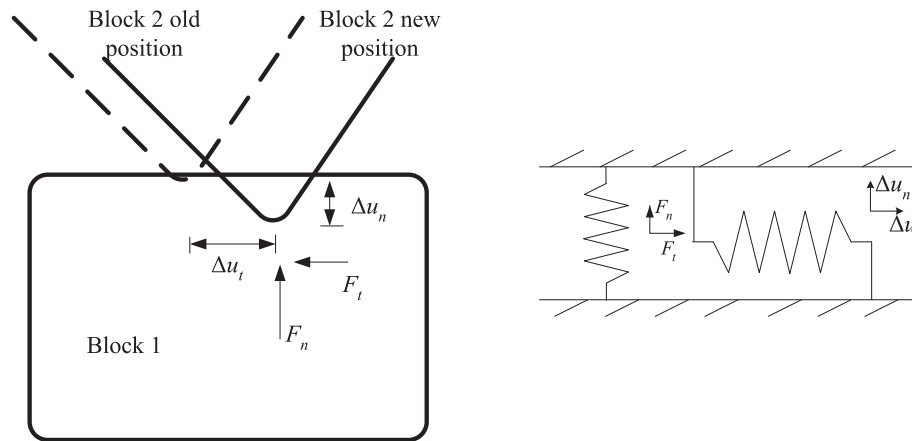


Fig. 3. Joint contact stiffness and overlap (adopted from Itasca, 2014).

in jointed rock is performed using the distinct element code UDEC. The UDEC model was developed based on the experimental shake table study of a tunnel in jointed rocks reported by Ahola et al. (1996). The model is in accordance with the rigid shake table apparatus of length 122 cm and breadth 122 cm, and extends to a depth of 61 cm. Two joint sets of 5 cm spacing dipping 45° in the clockwise and anticlockwise directions with the horizontal are present. A tunnel of diameter 15.2 cm is introduced at the center of the model. The top of the model is free, and the bottom and sides of the block are fixed to simulate a rigid shake table apparatus (Fig. 4). The ingots used in the shake table experiment are similar to a long beam element, and is continuous in the lateral direction. This agrees well with the UDEC model of the plane strain assumption.

In-situ stresses of 4.695 MPa and 10.941 MPa were applied in the horizontal and vertical directions, respectively. The material model is elastic to facilitate block displacements strictly by joint deformations, and the joints adhere to the Coulomb slip (Eqs. (7)–(9)) to allow the blocks to slide past each other. The properties of the model are given in Table 1 (Ahola et al., 1996; Kana et al., 1997). Each of the blocks has been meshed to triangular zones of size 1 cm. The joint properties used in UDEC modeling were obtained from the pseudostatic and cyclic shearing tests conducted on the joints by Kana et al. (1997) and Ahola et al. (1996).

The seismic loading was assigned a scaled value of the September 1985, Mexico City earthquake on the bottom and sides of the model, similar to that applied in the shake table experiment. Because the UDEC accepts only velocity, force, or stress as its input, the earthquake loading was applied as the velocity input. The recorded accelerogram of the 1985 Mexico earthquake is shown in Fig. 5(a). The acceleration time history for the earthquake motion was obtained from accelerograms of the Guerrero array, and the motion in the south direction as published by the COSMOS website was considered for the study. To understand the frequency content of the earthquake motion, Fourier spectra was obtained from the time history of acceleration,

which is shown in Fig. 5(b). It is found from the Fourier spectra that the frequency content of the input motion varies from 0.1 to 10 Hz, and the Fourier amplitude predominantly concentrates between 0.2 and 2 Hz. The fundamental frequency of a rocky terrain in general ranges between 3 Hz and 5 Hz, as reported by Zulficar, Alcik, and Cakti (2012). However, for a jointed slope, the fundamental frequency is found to be approximately 2 Hz according to Noorzad, Aminpur, and Salari (2008). Hence, the predominant frequency of the input motion is found to be close to the fundamental frequency of a typical jointed rocky terrain, thus rendering the considered model highly susceptible to the 1985 Mexico earthquake. The earthquake data for a bracketed duration starting from 15 s to 45 s were obtained when the earthquake was predominant. Because the study was conducted on a scaled model and not a field size model, the earthquake data for the bracketed duration were scaled down. The scaling down was performed according to a similitude ratio for 1 g by Iai (1989).

Figure 6(a) shows the velocity time history for the bracketed duration obtained from the time history of ground acceleration. Further, the corresponding displacement time history as obtained from the velocity time is shown in Fig. 7(a). The scaled-down value of the velocity and displacement for the bracketed duration are shown in Figs. 6(b) and 7(b), respectively. The scaled-down velocity time history as shown in Fig. 6(b) was applied as the input for the UDEC analysis. The shake table displacement as obtained during this input is shown in Fig. 7(b). This is similar to the shake table displacement given as the input in the laboratory experiment.

The model was first analyzed under static conditions before applying the earthquake input. To understand the threshold input displacement at which the block sliding was initiated, a number of loading cycles were imposed with different scaled input motions. Each value was repeated for four cycles. The maximum displacement of the shake table from its original position increased to 3.8 mm, 7.6 mm, 11.7 mm, and 15.5 mm. The deformations caused by the sliding along the joints were found to be

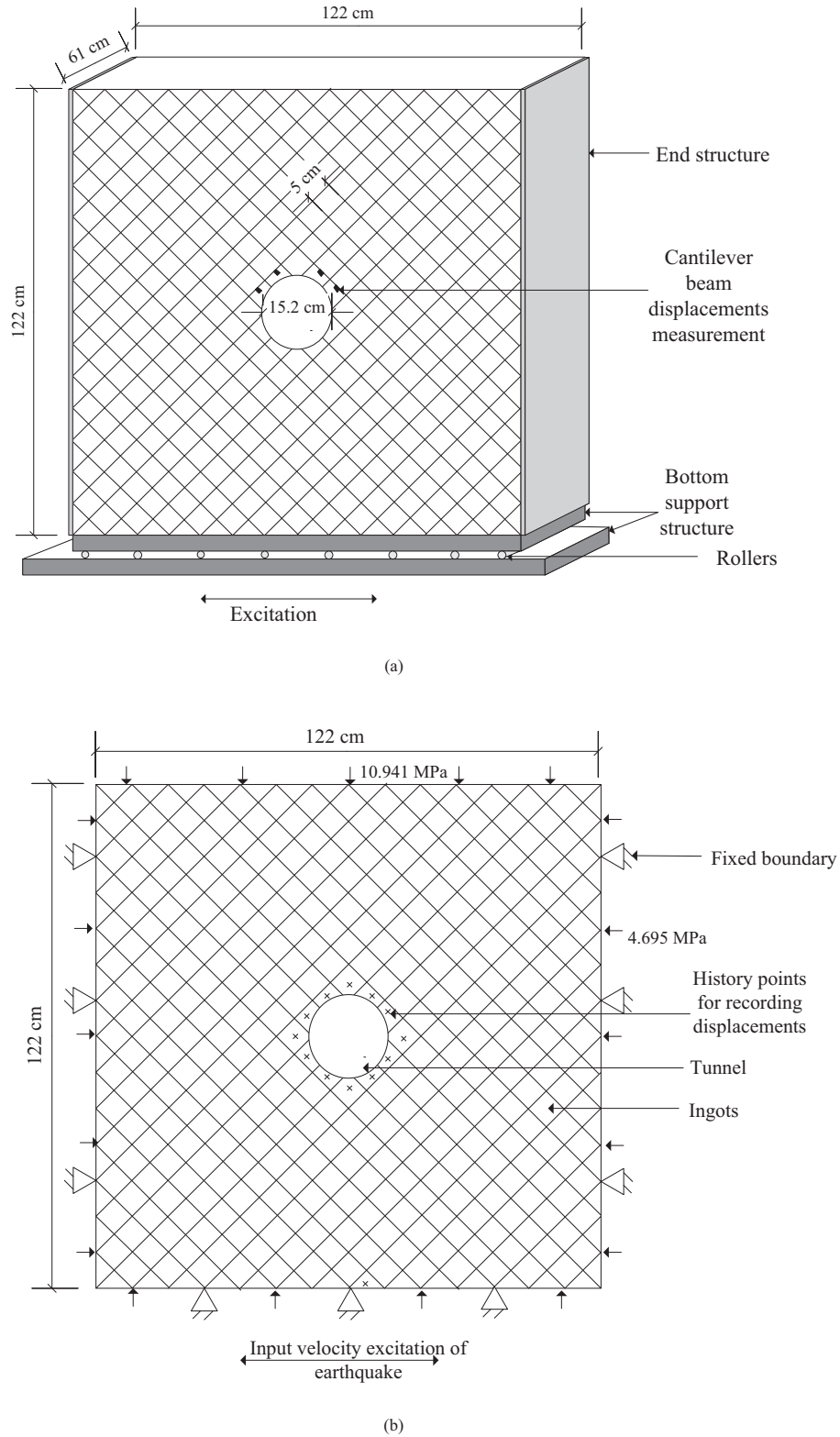


Fig. 4. Shake table: (a) Representative image for the shake table experiment (Ahola et al., 1996) and (b) Corresponding UDEC model.

cumulative, and threshold seismic displacement amplitude was identified. The deformations occurring around the tunnel are well beyond this threshold value. It was found to exceed 15.5 mm beyond the threshold in terms of the dis-

placement of the shaking table. During the application of earthquake loading, the deformations of the blocks in the tunnel periphery were recorded. Figure 8(a) shows the tunnel at the end of all loading cycles as obtained from UDEC

Table 1
Material properties of the rock and joints (Ahola et al., 1996).

Property	Values
Density (kg/m ³)	1 682
Bulk modulus (GPa)	0.145
Shear modulus (GPa)	0.129
Joint normal stiffness (GPa)	0.7
Joint shear stiffness (GPa)	0.5
Joint friction angle (°)	25.56

analysis. The displacement of the top left ingot as marked in Fig. 8(a) is compared with the displacement of the same ingot during experimental study is shown in Fig. 8 (b). It is found from Fig. 8(b) that blocks on the top-left of the tunnel are found to slip down 4.5 mm after the 15th cycle of loading with the displacement amplitude as 15.5 mm. The overall pattern of displacement is found to be similar but the peak displacement value in the UDEC is underestimated by 13%. However, the UDEC simulation can achieve the same threshold input value as that of the laboratory experiment.

4 Tunnel deformation under seismic loading

The joint behaviors are highly dependent on the properties of the medium as well as those of the joints. Therefore, understanding the effect of dynamic loads under different conditions is necessary. This UDEC study is extended to understand the effect of different combinations of in-situ stress, joint dip angle, joint stiffness, and joint friction angle on this circular tunnel, while the shake table test with earthquake motion is applied. In this study, the UDEC analysis of a tunnel in jointed rock is performed for a single cycle of the scaled Mexico earthquake loading lasting 10 s with a threshold displacement of 15.5 mm. The original shake table model contained two joints, both having a dip angle of 45° with the horizontal, one clockwise and another anticlockwise, in-situ stresses of 10 MPa and 4 MPa in the vertical and horizontal directions, respectively, joint normal stiffness of 0.7 GPa/m, and joint shear stiffness 0.5 GPa/m. Therefore, all the parameters were maintained the same as in the shake table study, and only the parameter under consideration was changed. In the study, a tunnel was considered to fail if a block underwent

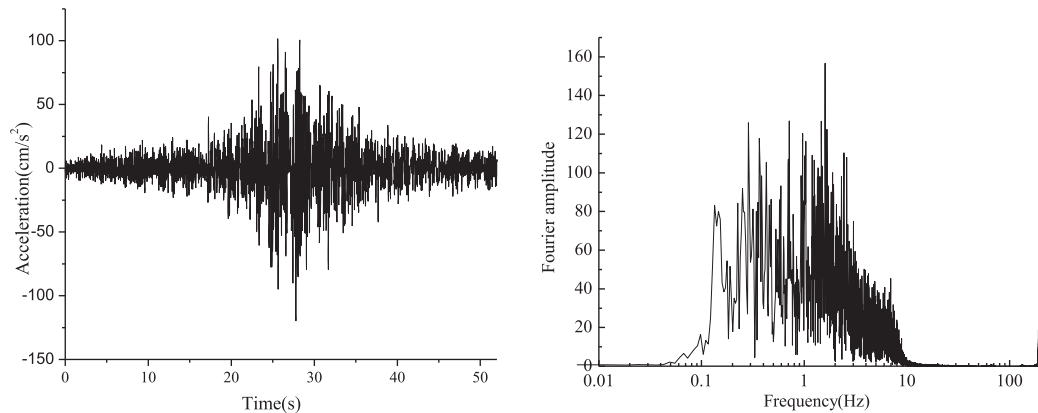


Fig. 5. (a) Time history of acceleration and (b) Fourier Spectra of recorded 1985 Mexico earthquake.

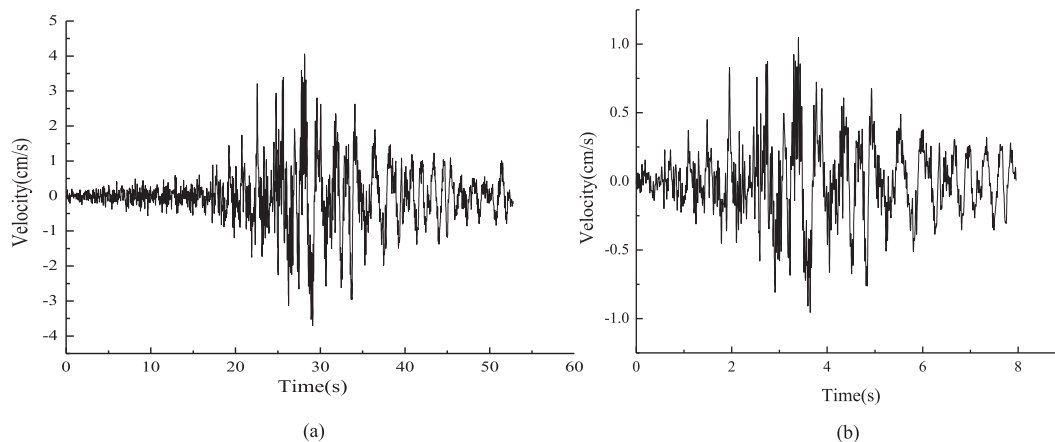


Fig. 6. Time history of velocity: (a) recorded and (b) scaled down 1985 Mexico earthquake.

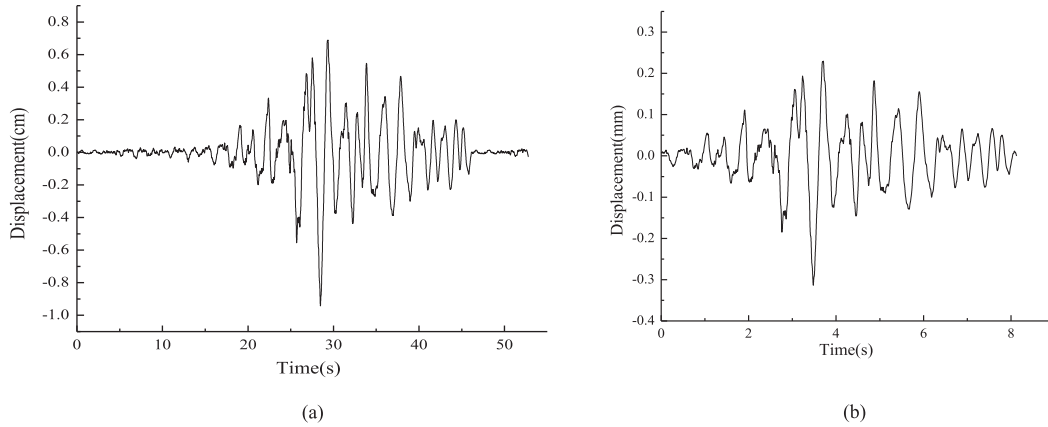


Fig. 7. Time history displacement: (a) recorded and (b) scaled down 1985 Mexico earthquake.

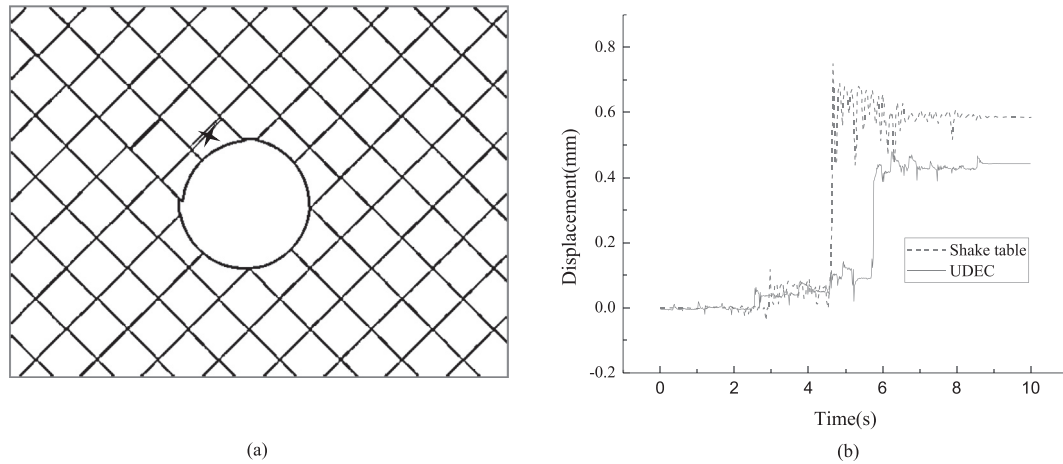


Fig. 8. (a) UDEC model at the end of the analysis (b) Comparison of displacements of the top left ingot in the experiment and in the UDEC analysis for the 13th cycle.

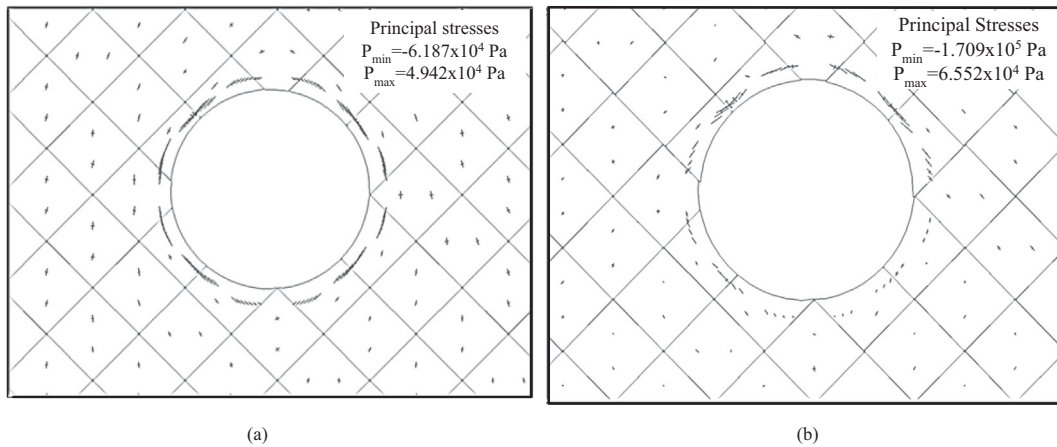


Fig. 9. Stress concentration around the tunnel after shake table study obtained from UDEC: (a) static and (b) dynamic.

destressing or joint slip occurred. The tunnel was considered to be unsupported owing to its high stability under static conditions.

Figure 9 shows the change in stress around the tunnel owing to static and dynamic loading. The joint slip and displacement can be observed on the sides of the crown block.

This is due to the presence of the shear zone around the tunnel in an X shape, as reported by Shen and Barton (1997), based on their study under static loading conditions. Under static condition, the stresses can be observed to be concentrated equally around the tunnel. However, additional stress concentrations around the tunnel after the application of dynamic load leads to stress redistribution. Nevertheless, the primary stress concentrations still adhere to the X shape. It is evident from the destressing that occurred by displacements in the ingot (Fig. 9(b)). This destressing is due to the increase in tensile stresses leading to an increase in the principal stress values after dynamic loading.

4.1 Effect of in-situ stress

The experimental study by Ahola et al. (1996) was performed for a scaled model representing a high in-situ stress in the field. However, under an urban scenario, where the tunnels are shallow, the in-situ stresses acting on the tunnels are low. To understand the behavior of jointed rock tunnels under all depths, the models were analyzed for other combinations of in-situ stresses. For a shallow depth, the horizontal stress may be high compared to the vertical stress. In other conditions, the horizontal stress may be lower than the vertical stresses, when a structure exists above the ground. Therefore, the importance of the effect of in-situ stress on the joints, and the portion of the tunnel experiencing problems can be understood by considering the in-situ stress effects. The study is performed with different combinations of horizontal and vertical stresses. The ratio of horizontal stress to vertical stress is called the lateral stress coefficient. Because the variation in change in the lateral stress coefficient is a representation of different stress combinations, the results are given in terms of the lateral stress coefficient.

Figure 10 shows the tunnel deformations under dynamic loading when the lateral stress coefficient is varied from 0.1 to 1 for various horizontal stress conditions. It is found that, as the lateral stress coefficient increases, the tunnel deformations increase. Although the pattern of stress variation is similar for all horizontal stress values, at lower stresses, the blocks are found to undergo maximum deformation. This might be because the blocks are relatively loose at the lower confinement. For a higher lateral stress coefficient, the deformations are lower for a given horizontal stress. Thus, the destressing would be more prominent under a higher lateral stress coefficient. However, as the horizontal stress increases, the total stresses acting on the blocks will be higher for the same lateral stress coefficient value, hence producing less displacement and higher stress concentration. The decrease in displacements around the tunnel with increasing in-situ stress can be explained by the effect of stresses owing to dynamic loading affecting less on the tunnel if it is approximately equal to or less than the existing stresses around the tunnel. Deng et al. (2014) also obtained similar findings for tunnel deformation under

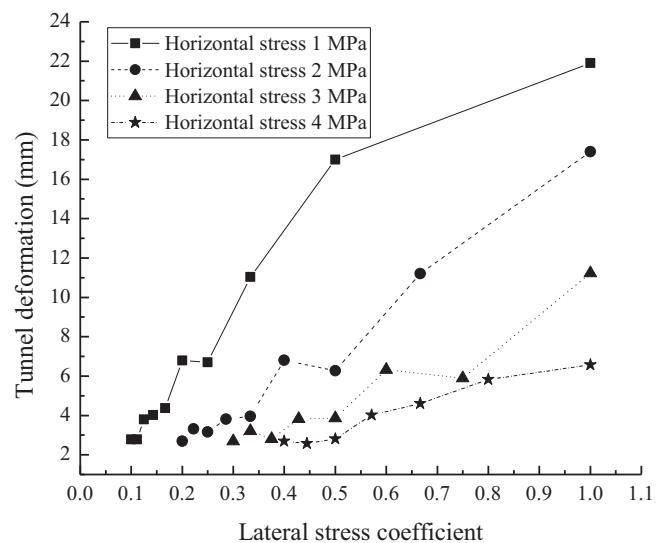


Fig. 10. Effect of lateral stress coefficient on tunnel dynamic deformation at different horizontal stress.

blast loading under different in-situ stress conditions. This implies that a tunnel at a shallow depth exhibits a higher failure risk than a deep-seated tunnel. This result agrees well with those of Hashash, Hook, Schmidt, and Yao (2001) and Deng et al. (2014). The maximum deformation with the present combination of stresses is found to be approximately 21 mm under the scaled earthquake load, whereas for static it is less than 0.3 mm. This accounts for 14% strain under dynamic loads and is an extremely high value.

4.2 Effect of joint properties

4.2.1 Joint angle

The joint angle is varied to understand the effect of joint dip on the tunnel deformation and its effect at the surface. The study was conducted for all possible joint combinations by maintaining the first joint angle and varying the second joint angle from 0° to 90° in the anticlockwise direction from the horizontal. The first joint angle was varied from 0° to 90° clockwise with the horizontal. Only joint angle variations from 0° to 90° were considered as the tunnel is circular and symmetric. Many blocks that are stable under static conditions had loosened and failed on the application of seismic load. Figures 11–14 show various joint combinations under static and dynamic loadings where the tunnels are stable under static loading (Figs. 11(a), 12(a), 13(a), and 14(a)) while it failed under the application of a dynamic load of the scaled 1985 Mexico earthquake (Figs. 11(b), 12(b), 13(b), and 14(b)). Figure 11 shows a tunnel in joint set with one angle of 40° and the other 0°. The tunnel stable under static conditions contained two key blocks from the side that moved out during dynamic loading. Figure 12(a) shows the tunnel with joint angle 40° and 10° stable under static loading. Figure 12(b) shows a large part of the tunnel from the left sidewall moving into

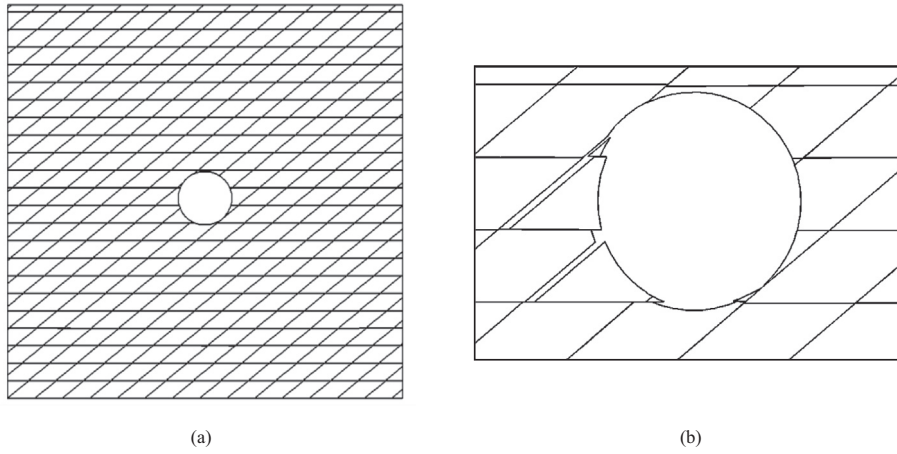


Fig. 11. Model for first joint angle 40° and second angle 0° after: (a) static loading and (b) dynamic loading as obtained from UDEC.

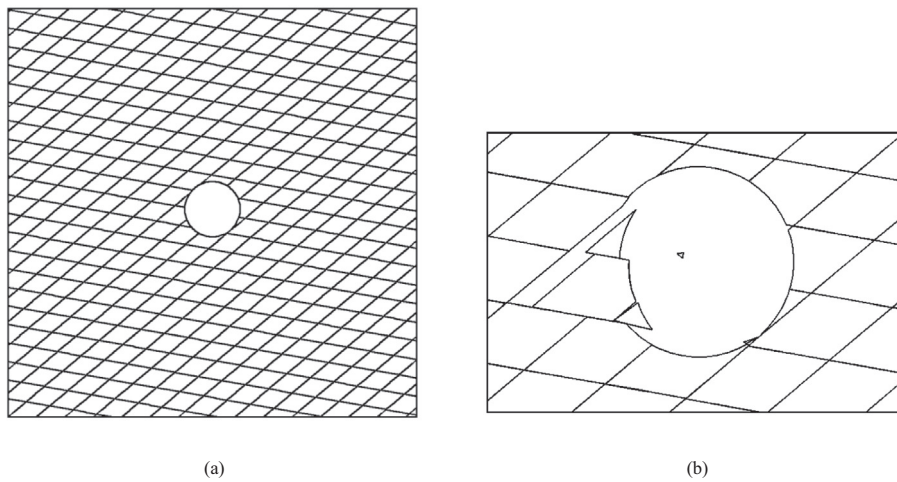


Fig. 12. Model for first joint angle 40° and second angle 10° after: (a) static loading and (b) dynamic loading as obtained from UDEC.

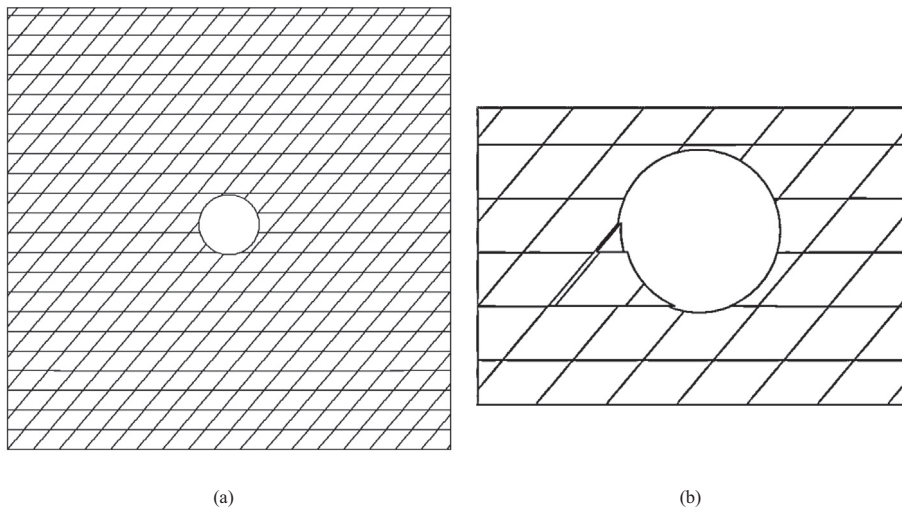


Fig. 13. Model for first joint angle 50° and second angle 0° after: (a) static loading and (b) dynamic loading as obtained from UDEC.

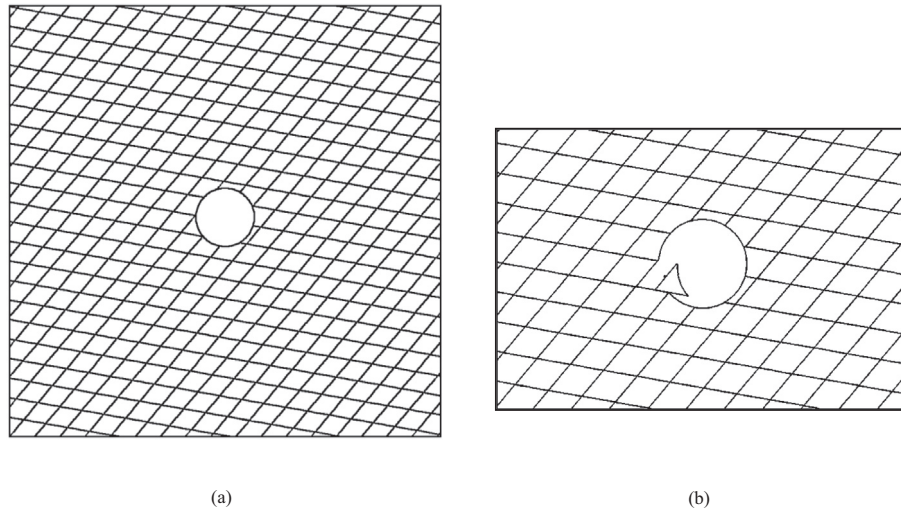


Fig. 14. Model for first joint angle 50° and second angle 10° after: (a) static loading and (b) dynamic loading as obtained from UDEC.

the tunnel. Figure 13(b) shows the failure of the tunnel with joint angles 50° and 0° under dynamic loading compared to a stable tunnel under static condition. The blocks on the left bottom adjoining the tunnel periphery are found to undergo destressing and move into the tunnel during the application of dynamic load. In Fig. 14(b), the tunnel in joint angles 50° and 10° contains a key block from the left tunnel wall that slide into the tunnel under the action of dynamic load.

In most cases, the simulation stops because of the joint overlap error that occurs during UDEC analysis. This occurs as the overlap between two blocks is higher than the permissible limit. In the actual field condition, this collision of blocks may also result in the breakage of blocks. In the study, the joint angles are found to undergo loosening or separation if one of the joint angles are approximately 40° and 60° with the horizontal. The maximum failure occurs when one angle is between 0° and 20° , while the second joint set is at an angle between 40° and 60° , thus creating a wedge for the block to slide. This may be because the slips along the joints are difficult when the angle created between the joints is less than the interjoint friction angle, which is equal to 35° in this case. Under these joint combinations, all the four angles in the blocks are greater than the joint friction angle. It is found that the left roof and sides of the tunnel experienced maximal deformation. Similar results were observed by Deng et al. (2014) in their study to understand the maximum peak particle velocity occurring at different parts of the tunnel for a blast occurring at the surface.

Only joint angle variations from 0° to 90° have been considered as the tunnel is circular and symmetric. Figures 15 and 16 show the surface settlement occurring under the action of dynamic load. Surface settlements are found to occur in most cases owing to the readjustment of blocks even though the displacement at the tunnel periphery is negligible. Readjustment in the blocks occurs as part of

the opening and closing of joints under the action of the dynamic load, as shown in Fig. 15. Figures 15 and 16 show that the maximum surface displacement may not always occur above the crown as it is dependent on the joint angle. The surface settlements and the opening of joints at different portions of the model occur owing to the rearrangement and slippage of blocks, even if no specific damage is observed around the tunnel. Settlements near the boundary were observed in most of the joint conditions. This is an effect of the boundary conditions and a drawback with laboratory or numerical modeling. Under field conditions, these boundary settlements will be continuous or stepped.

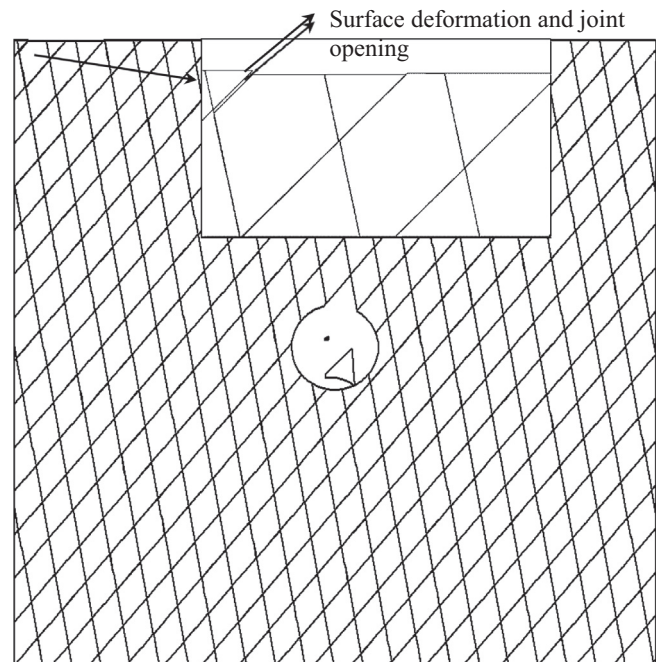


Fig. 15. Surface deformation and joint opening under the action of dynamic load when joint first joint angle is 50° and second is 80° as obtained from UDEC.

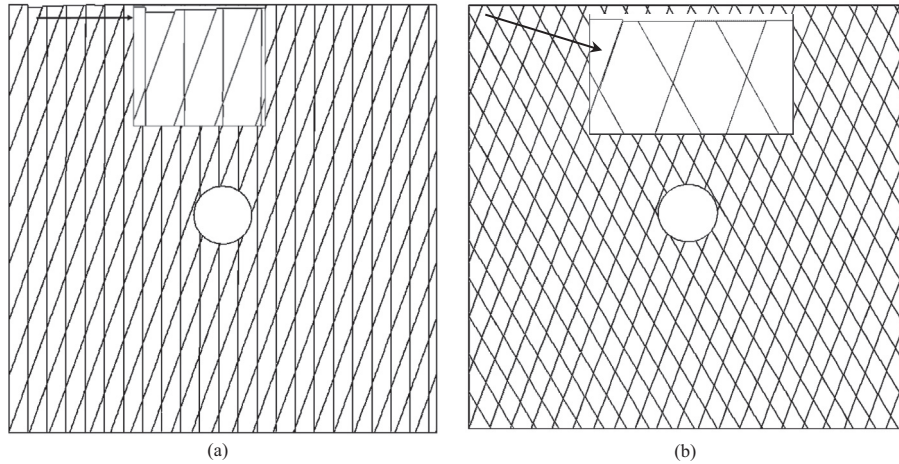


Fig. 16. Surface settlement with no tunnel deformation as obtained from UDEC: (a) first joint angle 90° and second 70° and (b) first joint angle 70° and second angle 60°.

4.2.2 Joint stiffness

Joint stiffness is an important aspect that determines the slippage between joints. The value of joint stiffness adopted in the numerical study is often higher than the elastic modulus of the intact rock itself. However, it is reasonable to use such a value, as the joint infilling material affects the joint stiffness value in the field that is not incorporated in the numerical model, as indicated by Deng et al. (2014). In this study, the effect of deformation with the variation in joint normal stiffness and joint shear stiffness is studied. The joint normal stiffness was varied from 0.3 GPa/m to 1 GPa/m without changing the original joint shear stiffness value of 0.5 GPa/m. Figure 17 shows the variation in tunnel deformation with various joint normal stiffness values, both for static and dynamic conditions. It is found from Fig. 17 that, as the joint normal stiffness increases, tunnel deformation decreases. The variation in joint normal stiffness

shows a direct relation with tunnel deformation. In the static case, the variation is primarily linear but when a dynamic load is applied, the deformation values decrease exponentially with the increase in joint stiffness, both at the tunnel periphery and surface. As the normal stiffness value is varied from 0.6 GPa/m to 1 GPa/m, the variation is comparatively small for static and dynamic loadings. However, for the variation from 0.3 GPa/m to 0.6 GPa/m, the variation in the maximum deformation is significant under dynamic loading. A peak displacement of 5 mm is observed under the dynamic condition for a normal stiffness of 0.3 GPa/m compared to a 0.5 mm deformation for the same stiffness under the static condition.

Figure 18 shows the variation in deformation corresponding to the change in joint shear stiffness. Subsequently, the joint shear stiffness is varied from 0.1 GPa/m to 1 GPa/m with a constant joint normal stiffness value

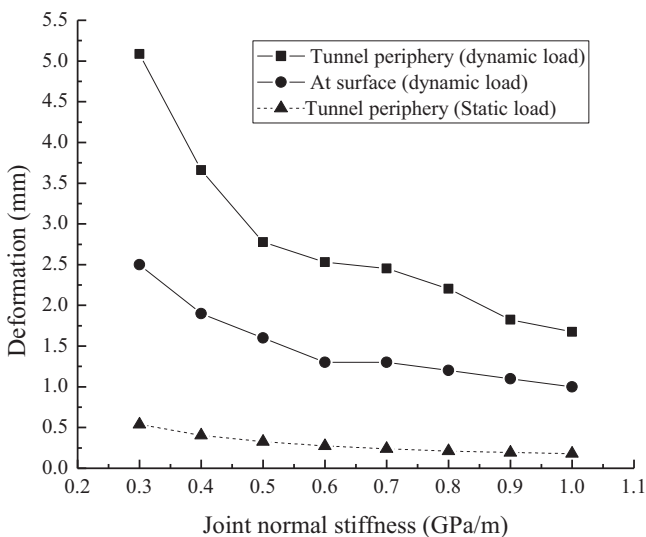


Fig. 17. Effect of joint normal stiffness on static and dynamic deformation of tunnels.

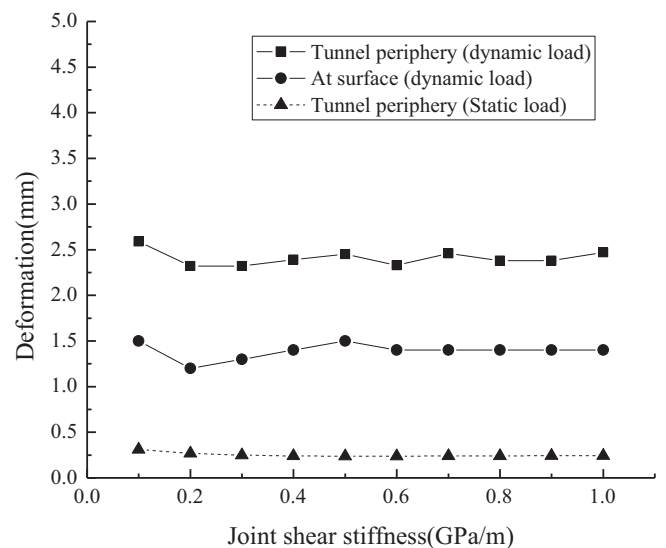


Fig. 18. Effect of joint shear stiffness on static and dynamic deformation of tunnels.

of 0.7 GPa/m. However, the variation in joint shear stiffness shows no considerable differences in the tunnel deformations both in the static and dynamic situations. This result corresponds to the UDEC theory of interaction forces and displacements (Eqs. (6) and (9)) during joint slippage. According to the theory, shear forces on the contact are influenced by the normal stiffness and friction angle. Similar results are reported by Yoo et al. (2017) for a single set of joints. Although the tunnel deformations demonstrate comparatively small effects with changes in shear stiffness, the increase in deformation under dynamic loading conditions shows an increase of 5 mm from 0.25 mm under static conditions around the tunnel. This accounts for approximately 3% strain with reference to the tunnel diameter. Although these displacements appear negligible in the scaled model, it corresponds to large displacements in the field. For the dynamic loading of a tunnel of 10 m diameter, for 3% strain, it will experience a 30-cm displacement of the blocks in dynamic loading from 1.6 cm under static conditions. This clearly shows the instability of the tunnel under earthquake loading.

4.2.3 Joint friction angle

The study is based on the tunnel deformation by inter-joint slip, where the interjoint friction is important. The variation in joint friction depends on the smoothness or roughness of the joints, and the presence of the infilling material. As the roughness decreases, the joint friction decreases, and the effect of this change in joint friction on the joint slip has been studied. The joint friction angle was changed from 18° to 38° assuming that the joint stiffness properties are not affected significantly in the ranges of friction angle values above. Figure 19 represents the change in tunnel deformation with change in friction angle for static and dynamic cases.

Figure 19 shows that under static and dynamic conditions, the tunnel deformation decrease linearly with

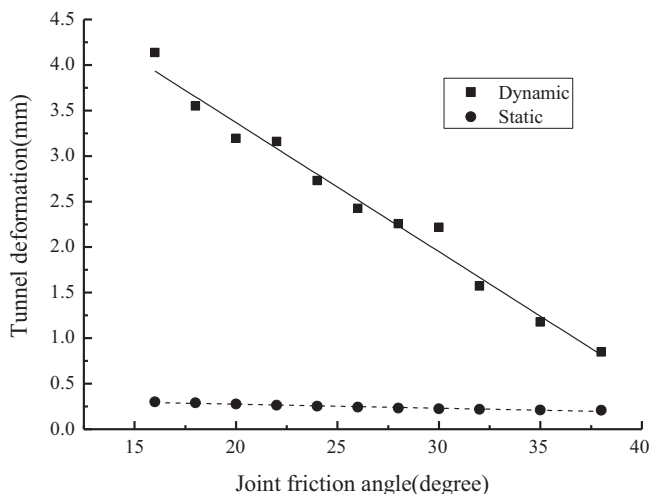


Fig. 19. Tunnel deformation under dynamic and static loading for various joint friction angles.

increasing joint friction angle. Because the deformation and failure allowed in the present study is only by joint slip, this directly reflects the effect of joint slippage with change in joint friction angle. This decrease is predominant in the case of dynamic loading compared to static loading conditions. The deformation slope in the case of dynamic loading is much higher compared to that of static loading, indicating a steep increase in deformation with decreasing angle of joint friction. The linear decrease is because the slippage is directly proportional to $\tan \varphi$. Further, the effect becomes more pronounced with the application of a dynamic load. The joint slip difference between the static and dynamic case is relatively lower at higher friction angles.

5 Summary and conclusions

A shake table experimental study on a tunnel in jointed rocks reported in the literature was simulated using the UDEC. The tunnel was subjected to a scaled input motion of the 1985 Mexican earthquake. The numerical results were validated with the findings of the shake table experiment. Further, the developed numerical model was used to perform parametric studies to understand the effect of in-situ stress, joint orientation, joint stiffness, and joint friction angle on the deformation and stability of the tunnel under the same earthquake input motion. Based on the numerical studies, the conclusions are as follows:

- (1) The joint displacements were found to be cumulative under dynamic loads, and the tunnel failed after a series of repetitive loading. This result agreed with the earlier study performed by Ma and Brady (1999), where the joints were analyzed using the Coulomb slip model and continuously yielding models.
- (2) A threshold amplitude of the dynamic load was identified above which the tunnel deformations were more profound.
- (3) Increase in tunnel deformations under seismic loading indicated that tunnels in jointed rocks were highly susceptible to earthquake loads. The tunnel deformation under static conditions was less than 0.3 mm; however, under the action of dynamic load, a considerable increase in tunnel deformations were observed, leading to complete failure in some cases.
- (4) Deformations around the tunnel increased with increasing lateral stress coefficients. For the same lateral stress coefficient, a lower horizontal stress produced higher deformations. This implies that a tunnel at a shallow depth exhibits a higher risk of failure than deep tunnels.
- (5) The joints that were stable under static conditions failed under seismic loading, specifically for some joint angle combinations. The joint angles underwent loosening or separation, if one of the joint angles were approximately 40° and 60° with the horizontal. Maximal failure occurred when one angle was

between 0° and 20°, while the second joint set at an angle between 40° and 60° formed a wedge for the block to slide.

- (6) Under dynamic loads, with increasing joint normal stiffness, the tunnel deformations decreased exponentially unlike a linear decrease under the static case. The difference in tunnel deformation under dynamic loading and static loading was significantly lower when the joint stiffness value was beyond 0.6 GPa/m. This difference in the deformation behavior between static and dynamic loading was high when the joint stiffness was between 0.3 GPa/m to 0.6 GPa/m.
- (7) With decreasing joint friction angle, the joint slip increased linearly. This increase was more profound under dynamic conditions compared to static conditions. The difference between the static and dynamic cases reduced for higher friction angles.
- (8) Tunnel deformation values observed under dynamic loads were in the laboratory scale and accounted for 2%~5% strain with reference to the tunnel diameter. This value may be considered significant for the field tunnels.
- (9) The opening and closing of joints at different points of the rock mass, even if not exactly at the tunnel opening, resulted in possible slippage and strength losses.

A few limitations considered important for this analysis are as follows:

- (1) The maximum displacement at the surface was observed next to the boundary of the model and decreased toward the center of the model. The boundary effect may act as a determining criterion for the present response and was different from that of the actual boundary conditions.
- (2) The contact overlap error occurred in many of the analyses. This is a representation of fatigue failure at the joints, as reported by [St. John and Zahrah \(1987\)](#). Because the model could not simulate this failure of one joint crashing against another joint thus causing breakage, the contact overlap error was introduced.

The study highlights the strength reduction and instability occurring on rocks because of joints and the corresponding effect with respect to tunnels. The effect of supporting elements for the tunnel has not been considered in the study, and a detailed study on the contributing effect of tunnel supports during seismic loading is under investigation.

Conflict of Interest

The authors wish to confirm that there are no known conflicts of interest associated with this publication and

there has been no significant financial support for this work that could have influenced its outcome.

Acknowledgment

The authors acknowledge the suggestions of Dr. Wesley Patrick, Center for Nuclear Waste Regulatory Analyses (CNWRA[®]) at Southwest Research Institute[®] (SWRI[®]), USA.

References

- Abokhalil, M. (2007). Insights into the response of rock tunnels to seismicity. Master's Thesis in Geosciences, Department of Geosciences, University of Oslo.
- Adyan, Ö., & Kawamoto, T. (2004). The damage to lignite mines caused by the 2003 Miyagi-Hokubu earthquake and some considerations on its causes. In 3rd Asian rock mechanics symposium, Kyoto (Vol. 1, pp. 525–530).
- Adyan, Ö., Shimizu, Y., & Karaca, M. (1994). The dynamic and static stability of shallow underground openings in jointed rock masses. In The 3rd int. symp. on mine planning and equipment selection, Istanbul (pp. 851–858).
- Adyan, Ö., Ohata, Y., Genis, M., Tokashiki, N., & Ohkubo, K. (2010). Response and stability of underground structures in rock mass during earthquakes. *Rock Mechanics Rock Engineering*, 43, 857–875.
- Ahola, M. P., Hsuing, S. M., & Kana, D. D. (1996). Experimental study on dynamic behavior of rock joints. Coupled thermo-hydro-mechanical process of fractured media. *Developments in Geotechnical Engineering*, 79, 467–506.
- Barton, N. (1984). Effects of rock mass deformation on tunnel performance in seismic regions. *Advances in Tunnelling Technology and Subsurface Use*, 4(3), 89–99.
- Cundall, P.A. (1971). A computer model for simulating progressive large scale movements in blocky rock systems. In Proceedings of the symposium of the international society of rock mechanics, society for rock mechanics (ISRM), France (Vol. 1), Paper No. II-8.
- Deng, X. F., Zhu, J. B., Chen, S. G., Zhao, X. Y., Zhou, Y. X., & Zhao, J. (2014). Numerical study on tunnel damage subject to blast-induced shock wave in jointed rockmasses. *Tunnelling and Underground Space Technology*, 43, 88–100.
- Dhawan, R. K., Singh, D. N., & Gupta, I. D. (2004). Dynamic analysis of underground openings. *Rock Mechanics and Rock Engineering*, 37(4), 299–315.
- Dowding, C. H., & Rozen, A. (1978). Damage to rock tunnels from earthquake shaking. *Journal Geotech Engineering Division, ASCE, GT2*, 175–191.
- Genis, M., & Adyan, Ö. (2002). Evaluation of dynamic response and stability of shallow underground openings in discontinuous rock masses using model tests. In Proc. of 2002 ISRM regional symposium (3 rd Korea-Japan joint symposium) on rock engineering problems and approaches in underground construction, Seoul (Vol. 2, pp. 787–794).
- Hart, R. D. (1993). An introduction to distinct element modelling for rock engineering. In *Analysis and Design Methods* (pp. 245–261). Pergamon Press, Oxford.
- Hashash, Y. M. A., Hook, J. F., Schmidt, B., & Yao, J. I. (2001). Seismic design and analysis of underground structures. *Tunnelling and Underground Space Technology*, 16, 247–293.
- Heuze, F. E., & Morris, J. P. (2007). Insights into ground shock in jointed rocks and the response of structures there-in. *International Journal of Rock Mechanics and Mining Sciences*, 44, 647–676.
- Iai, S. (1989). Similitude for shake table tests on soil-structure-fluid model in 1g gravitational field. *Soils and Foundations*, 29, 105–118.
- Itasca Consulting group Inc. (2014) UDEC User Manuals.
- Kana, D. D., Vanzant, B. W., Nair, P. K., & Brady, B. H. G. (1991). Critical assessment of seismic and geomechanics literature related to a high-level nuclear waste underground repository. USA. doi: 10.2172/138128.
- Kana, D. D., Fox, D. J., Hsuing, S., & Chowdhury, A. H. (1997). An experimental scale model study of seismic responses of an underground opening in jointed rock mass. USA. doi: 10.2172/464193.

- Kaneshiro, J. Y., Power, M., & Rosidi, D. (2000). Empirical correlations of tunnel performance during earthquakes and a seismic aspects of tunnel design. In Proceedings of the conference on lessons learned from recent earthquakes on earthquakes in Turkey.
- Ma, M., & Brady, B. H. (1999). Analysis of the dynamic performance of an underground excavation in jointed rock under repeated seismic loading. *Geotechnical and Geological Engineering*, 17, 1–20.
- Noorzad, A., Aminpur, M., & Salari, H. (2008). Seismic slope stability analysis of jointed rock masses on the northern abutment of Gotvand dam, Iran. In The 14th world conference on earthquake engineering, October 12–17, 2008, Beijing, China.
- Owen, G. N., & Scholl, R. E. (1981). Earthquake engineering of large underground structures. NASA STI/Recon Technical Report No. FHWA_RD-80_195. Federal Highway Administration and National Science Foundation.
- Power, M. S., Rosidi, D., & Kaneshiro, J. (1998). Seismic vulnerability of tunnels and underground structures revisited. In Proc. North American Tunneling 98, Balkema, Rotterdam.
- Rosengren, L. (1993). Preliminary analysis of the dynamic interaction between Norrra Lanken and a subway tunnel for Stockholm, Sweden. *Tunnelling and Underground Space Technology*, 8(4), 429–439.
- Sharma, S., & Judd, W. R. (1991). Underground opening damage to underground facilities. *Engineering Geology*, 30, 263–276.
- Shen, B., & Barton, N. (1997). The disturbed zone around the tunnels in jointed rockmass. *International Journal of Rock Mechanics and Mining Sciences*, 34(1), 117–125.
- St. John, C. M., & Zahrah, T. F. (1987). Aseismic design of underground structures. *Tunneling Underground Space Technology*, 2, 165–197.
- Wang, Z. L., Li, Y. C., & Shen, R. F. (2007). Numerical simulation of tensile damage and blast crater in brittle rock due to underground explosion. *International Journal of Rock Mechanics and Mining Sciences*, 44(5), 730–738.
- Yoo, J. K., Park, J. S., Park, D., & Lee, S. W. (2017). Seismic response of circular tunnels in jointed rock. *KSCE Journal of Civil Engineering*, 22(2), 1–9.
- Zulficar, A. C., Alcik, H., & Cakti, E. (2012). Analysis of earthquake records of Istanbul earthquake rapid response system stations related to the determination of site fundamental frequency. In Proceedings of 15th world conference on earthquake engineering, Lisbon, Portugal (Vol. 36, pp. 28769–28776).